LBL-22513
Preprint

Lawrence Berkeley Laboratory
UNIVERSITY OF CALIFORNIA

EARTH SCIENCES DIVISION

RECEIVED
LAWRENCE
BERKELEY LABORATORY

FEB 20 1987

LIBRARY AND
DOCUMENTS SECTION

Submitted to International Journal of Heat and Mass Transfer

AN ANALYTICAL SOLUTION FOR HEAT TRANSFER AT A MOVING BOILING FRONT

K. Pruess, C. Calore, R. Celati, and Y.S. Wu

January 1987

TWO-WEEK LOAN COPY
This is a Library Circulating Copy
which may be borrowed for two weeks.

Prepared for the U.S. Department of Energy under Contract DE-AC03-76SF00098

LBL-22513 c.2

DISCLAIMER

This document was prepared as an account of work sponsored by the United States Government. While this document is believed to contain correct information, neither the United States Government nor any agency thereof, nor the Regents of the University of California, nor any of their employees, makes any warranty, express or implied, or assumes any legal responsibility for the accuracy, completeness, or usefulness of any information, apparatus, product, or process disclosed, or represents that its use would not infringe privately owned rights. Reference herein to any specific commercial product, process, or service by its trade name, trademark, manufacturer, or otherwise, does not necessarily constitute or imply its endorsement, recommendation, or favoring by the United States Government or any agency thereof, or the Regents of the University of California. The views and opinions of authors expressed herein do not necessarily state or reflect those of the United States Government or any agency thereof or the Regents of the University of California.

LBL-22513

An Analytical Solution for Heat Transfer at a Moving Boiling Front

by

K. Pruess[*], *C. Calore*[†], *R. Celati*[†], *and Y. S. Wu*[*]

[*]Earth Sciences Division, Lawrence Berkeley Laboratory,
University of California, Berkeley, California 94720

[†] Istituto Internazionale Per Le Ricerche Geotermiche
Consiglio Nazionale Delle Ricerche
Piazza Solferino 2, 56100 Pisa, Italy

January 1987

This work was supported by the U.S. Department of Energy, Geothermal Technology Division, under Contract No. DE-AC03-76SF00098, and by the Progetto Strategico Valorizzazione Materie Prime Minerali, CNR, Italy.

ABSTRACT

A problem of current interest in geothermal energy extraction is the injection of cold water into a porous medium containing superheated vapor. Such injection will cause a boiling front to move away from the injection point. When flow is approximated as being one-dimensional radial, it can be shown from similarity variable concepts that temperature, pressure, and boiling rate at the front are constant, independent of time. From heat and mass balance considerations an analytical solution is obtained for front temperature and evaporation rate. Comparison with detailed numerical simulations of the injection process shows excellent agreement.

NOMENCLATURE

b	boiling fraction, $b = q_{vf}/q_l$
C	specific heat
D	coefficient in pressure solution, defined in Equation (A.10)
Ei	exponential integral
f	increment factor for numerical grid (Table 2)
F	mass flux
h	specific enthalpy
H	formation thickness
k	absolute permeability
m	molecular weight of water
M	mass
n	number of moles present
p	pressure
q	mass flow rate
r	radial distance from injection well
R	universal gas constant
t	time
T	temperature
u	specific internal energy

V volume

x similarity variable, $x = r^2/t$

Z real gas compressibility factor

Greek Symbols

α diffusivity parameter for vapor flow, defined in Equation (A.5)

μ dynamic viscosity

ρ fluid density

$\overline{\rho}$ average fluid density

ϕ porosity

ω retardation factor for thermal front, defined in Equation (1)

Subscripts

o initial value

f relating to boiling front

h hot (at initial temperature)

inj injection

l liquid water

R rock

sat at saturation (vapor-liquid equilibrium)

v vapor

1.0 Introduction

Coupled processes of heat and multi-phase mass transfer in permeable media are encountered in many systems of interest in energy recovery or industrial applications. These processes are highly non-linear and can often be quantitatively described only by means of computer simulation. Often this is a rather cumbersome process involving hard-to-check approximations regarding space-and-time discretization and the propagation of sharp fronts. Therefore, considerable efforts are being made to develop analytical or semi-analytical solutions for special cases which, where feasible, provide an economy and accuracy of solution seldom attainable from numerical simulation [1-9]. Furthermore, independently obtained solutions can serve as a check on the accuracy of complex numerical simulators.

The present paper is concerned with a two-phase fluid and heat transfer problem that arises when cold geothermal waste fluids are injected into depleted reservoir zones containing superheated vapor [10-12]. We will make the approximation of considering horizontal flow only. Vertical flow effects may be important in some applications; these will be studied in a separate paper (in preparation). The mass- and energy-balance equations for one-dimensional radial flow of single-component two-phase fluid in a porous medium have been discussed in [3,5]. It was pointed out by O'Sullivan [5] that these equations admit a solution in terms of a similarity variable $x = r^2/t$, even when all non-linearities of two-phase flow are taken into account, provided that initial and boundary conditions, and sink and source rates, are prescribed in such a way that they can be expressed as functions of x. An important special case where this is possible is for a well flowing at a constant rate in an infinite system initially at uniform conditions of pressure, temperature, and saturation. In the similarity variable approach, the partial differential equations for mass- and heat-flow are reduced to

ordinary differential equations, which can be integrated with standard methods [13]. O'Sullivan and Pruess [3] presented similarity solutions for constant-rate injection into single-phase liquid and two-phase conditions. O'Sullivan [5] developed solutions for constant-rate production from single-phase liquid and two-phase conditions.

In this paper we study the injection of cold water into a porous medium containing vapor at low pressure (strongly superheated). We are mainly interested in the rate at which injected water vaporizes, and in the pressure and temperature conditions at the evaporation front. We show that these aspects of the problem can be solved analytically. In arriving at the analytical solution we need to invoke similarity variable concepts; however, it is not necessary to actually integrate the ordinary differential equations in the similarity variable x.

2. Cold Water Injection

The thermal conditions arising when cold water is injected into a porous medium containing hot water in single phase conditions are well known [14]. A cold front with temperature equal to injection temperature will advance from the injection point. Because of heat conduction effects the transition from injection temperature to original reservoir temperature will occur over a finite distance in the direction of flow; however, when heat conduction is neglected the thermal front is completely "sharp", with temperature making a finite jump from T_{inj} to T_o.

The thermal front is retarded in comparison to the hydrodynamic front because of heat exchange with the solid skeleton. Bodvarsson [14] showed that the retardation factor (ratio of cold volume to total swept volume) is

$$\omega = \frac{\phi C_{l,h}\, \rho_{l,h}}{(1-\phi)\rho_R C_R + \phi \rho_{l,h} C_{l,h}} \tag{1}$$

Conditions are considerably more complex when cold water is injected into a porous medium containing superheated vapor (see Fig. 1). The advancement of the cold front in this case will still be retarded from heat exchange with the solid, but it is clear that the liquid water outside the cooled region cannot be at original reservoir temperature. Liquid water can exist at temperature T_o only if pressure $p \geq p_{sat}(T_o)$; however, because initial pressure $p_o < p_{sat}(T_o)$, this would give rise to vigorous vaporization. As a consequence pressure would rise above p_o, while temperature would decline below T_o as heat would be transferred from the rock to boil fluid. Calore et al. [15] performed numerical simulations of this process and observed that pressure- and temperature-conditions at the vaporization front tend to stabilize, such that $p_o < p_f < p_{sat}(T_o)$. The rate at which vapor can flow away from the boiling front increases with p_f. However, because of the boiling conditions there is a one-to-one correspondence between front temperature

T_f and pressure p_f, namely, $p_f = p_{sat}(T_f)$. Therefore, when p_f increases so does T_f. This in turn will diminish heat transfer from the rock to the fluid, which depends on the temperature difference $T_o - T_f$. Conditions at the front stabilize at intermediate values of (p_f, T_f) in such a way that the rate of boiling from rock-fluid heat transfer equals the rate of vapor flow away from the front.

Several important conclusions regarding this process can be reached simply by recognizing that in an infinite system with uniform initial conditions and constant injection rate, conditions in the system depend on time and distance only through the similarity variable $x = r^2/t$. Therefore, the boiling front must occur at a fixed value $x = x_f$ and, furthermore, temperature and pressure at the front are time-independent. Behind the front we clearly must have $p > p_f$, because a finite pressure gradient is required to drive fluid to the front. From a physical viewpoint it is clear that temperature behind the front cannot exceed temperature at the front. From $p > p_f$ and $T \leq T_f$ we can conclude that the fluid behind the front must be in single-phase liquid conditions. Therefore, the boiling front is "sharp" and there is no extended two-phase zone. It should be noted that the sharp boiling front arises from the idealization made in a porous medium description, namely, that there is complete thermodynamic equilibrium locally between rocks and fluid. Even in fine-grained materials there will be a finite time for this thermal equilibration, so that in reality the boiling front would always be associated with a two-phase zone of finite width.

Finally, from the existence of the similarity variable it is clear that the boiling rate at the front is constant, independent of time.

3. Mathematical Treatment

In order to establish the thermodynamic conditions at the front, we need to consider pressure-driven flow of vapor away from the front, as well as temperature-driven flow of heat from the rock to the advancing liquid injection plume. As shown in Appendix A, the vapor flow leads to the following pressure condition.

$$p_f^2 = p_o^2 - \frac{ZRT_o\mu_v q_{vf}}{2\pi kHm} \exp\left(\frac{r_f^2}{4\alpha t}\right) \mathrm{Ei}\left(\frac{-r_f^2}{4\alpha t}\right) \tag{2}$$

Heat flow at the front is considered in Appendix B. Taking into account that temperature and pressure at the front must be related by the vapor pressure relationship for water we have from Equation (B.6).

$$p_f = p_{sat}(T_f) = p_{sat}\left(T_o - \frac{h_{vl}\,\phi\overline{\rho}_l}{(1-\phi)\rho_R C_R(q_l/q_{vf} - 1)}\right) \tag{3}$$

Equations (2) and (3) represent two non-linear coupled equations for the unknowns p_f (or, equivalently, T_f) and q_{vf}, which can be solved by means of Newton-Raphson iteration. Note that the parameters α and $\overline{\rho}_l$ appearing in these equations also depend upon p_f (or T_f), see equations (A.5) and (B.4). To solve equations (2) and (3) we have written a computer program which performs an "inner" iteration on (3), nested within an "outer" iteration on (2). The saturated vapor pressure relationship as well as all other thermophysical properties of water and vapor are taken from the steam table equations as given by the International Formulation Committee [16]. The exponential integral appearing in Equation (2) was evaluated using the approximation given in [13]. The iteration procedure is started by picking an initial guess $b^{(0)}$ for the boiling fraction $b = q_{vf}/q_l$. For this fixed $b^{(0)}$ Equation (3) is solved iteratively for $T_f^{(1)}$ and $p_f^{(1)}$, taking $T_f^{(0)} = T_o$ as starting guess. Having obtained $(p_f^{(1)}, T_f^{(1)})$ for boiling fraction $b^{(0)}$, a second solution of (3) is generated for $b^{(0)}+\delta b^{(0)}$, where $\delta b^{(0)}$ is a small

increment, $\delta b^{(0)} = 10^{-10} \cdot b^{(0)}$ say. This is needed for numerically computing derivatives in the subsequent Newton-Raphson process on (2), which gives a $b^{(1)} = b^{(0)} + \Delta b^{(1)}$. Subsequently another inner iteration is performed to obtain $(p_f^{(2)}, T_f^{(2)})$ pertaining to $b = b^{(1)}$ etc., the process being continued until the residuals of Equations (2) and (3) (i.e., the difference between left and right hand sides) are reduced to a small fraction (10^{-10}) of the left hand sides. The process usually requires 4-6 iterations for convergence. All calculations were done in double precision (128 bit word length), because among other things we require accurate numerical derivatives of water heat capacity, which itself is obtained as a numerical derivative of internal energy.

4. Results

From Equations (2) and (3) it is clear that boiling fraction b and front temperature T_f depend upon injection rate only through the group $q_l / k \cdot H$. Another strong parametric dependence occurs for porosity, ϕ, while dependence upon injection temperature is only present through $\overline{\rho}_l$, and is rather weak. Dependence upon initial reservoir pressure is also weak as long as $p_o << p_f$. A stronger dependence is present for initial reservoir temperature T_o.

We have generated solutions of Equations (2) and (3) for a range of "specific injection rates" $q_l / k \cdot H$ and reservoir porosities ϕ. All other parameters were held constant at values typical for the upper depleted zones of the Larderello field [15] (see Table 1). Results for boiling fractions and boiling front pressures and temperatures are presented in Figures 2 and 3. We observe that boiling fraction diminishes with increasing porosity, and with increasing injection rate. Vaporization is larger for smaller porosity as expected. Boiling front temperature is lower for larger vaporization rate.

5. Comparison with Numerical Simulations

We have numerically simulated the process of cold water injection into a superheated vapor zone, using the multi-phase multi-component fluid and heat flow simulator MULKOM [17]. MULKOM solves discretized approximations to the equations for mass and energy transport in porous media over finite subdomains [18]. The governing equations have been given in [19]. The finite difference method used in MULKOM can represent sharp fronts only in an approximate fashion [20,21]. A finite subdomain containing partly single-phase liquid, and partly single-phase vapor, will be represented as being in two-phase conditions because of volume averaging. Discretization errors can be particularly severe in problems with coupled thermal and phase fronts [22], and space- and time-truncation errors need to be scrutinized carefully so that acceptable results may be obtained.

In the simulations we employed a relatively fine grid near the injection point to resolve the thermal and phase fronts there (see Table 2). For $r > 100$ m grid spacing was increased logarithmically out to a total radius of $r = 25$ km, so that the system would be infinite-acting over the time periods simulated. Temperature- and phase-changes remained confined to the finely discretized region $r < 100$ m. Calculations were made with different time step sizes to check and control time truncation errors.

Before presenting results of the simulations we wish to discuss how a phase boundary is propagated in the finite-difference approximation. Consider a finite subdomain ("grid block") which initially contains single-phase vapor. As liquid water enters the grid block it is vaporized, so that pressure increases while temperature declines (see Fig. 4). Eventually pressure reaches the saturated vapor pressure at prevailing temperature, at which point the entire grid block makes a transition to two-phase conditions. Liquid continues to enter the grid block,

vaporizing in part. The heat of vaporization is being supplied by the porous medium, whose temperature declines in the process. Pressure must also decline, as in two-phase conditions it is being maintained at the saturation pressure for given temperature. The liquid entering the grid block is vaporized only in part, so that liquid saturation builds up until, eventually, the block makes a transition to single-phase liquid conditions. The process is then repeated at the next downstream grid block.

In order to make the simulations comparable with the analytical treatment heat conduction was neglected. Test calculations showed conduction effects on boiling front temperature to be negligibly small (of the order of 1 °C or less).

In Figure 5 we have plotted simulated temperatures as function of the similarity variable $x = r^2/t$, for the case $\phi = 8\%$; $q_l = 27.8$ kg/s, using simulated data at three different times varying by factors of approximately 10 and 100, respectively. The data clearly confirm the invariance with respect to r^2/t, but they also show considerable numerical dispersion and discretization effects, especially at the front between cold and hot single-phase liquid ($r^2/t = 8 \times 10^{-5}$ m^2/s).

The simulated volume of liquid in the injection plume (for $\phi = 8\%$, $q_l = 27.8$ kg/s) is compared in Figure 6 with the prediction from the analytical model (using Eq. (B.3) and our analytically calculated vaporization rate). The agreement is excellent. Simulated results for additional cases are shown in Figure 2; the agreement with the analytical predictions is good throughout.

It was discussed above how simulated pressures and temperatures at the boiling front go through a complex cycle in each grid block (see Fig. 4). To make a comparison with the analytical predictions we have calculated average pressures $\overline{p}_f$ for the entire period of two-phase conditions in a grid block. The points

labeled "numerical simulations" in Figure 3 show the saturated vapor temperature $T_f = T_{sat}(\overline{p_f})$ corresponding to the average simulated pressure at the front. Agreement with the analytical solution is good.

6. Conclusion

We have developed an approximate analytical solution for temperature (or pressure) and vaporization rate at a moving boiling front. The accuracy of the solution was confirmed by means of numerical simulations of cold water injection into a porous medium containing superheated vapor. The analytical solution should be useful in the design of geothermal injection systems, and for evaluating the accuracy of numerical solution techniques for multi-phase fluid and heat flow.

ACKNOWLEDGEMENT

This work was supported by the U.S. Department of Energy, Geothermal Technology Division, under Contract No. DE-AC03-76SF00098, and by the Progetto Strategico Valorizzazione Materie Prime Minerali, CNR, Italy. The authors would like to thank C. Doughty and C. F. Tsang for their careful review of this paper, and for suggesting improvements. For assistance in the preparation of the manuscript the authors are indebted to L. Fairbanks and D. Swantek.

REFERENCES

1. S. K. Garg, Pressure transient analysis for two-phase (liquid water/steam) geothermal reservoirs. Paper SPE-7479, presented at 53rd Annual Fall Technical Conference and Exhibition of the SPE, Houston, TX, October 1978.

2. Y. Ogniewicz and C. L. Tien, Porous heat pipe. *Heat Transfer, Thermal Control, and Heat Pipes,* Walter B. Olstad, ed., *Progress in Astronautics and Aeronautics,* Vol. 70, Martin Summerfield, series ed., presented at AAIA Thermophysics Conference, Orlando, Florida, June 1979.

3. M. O'Sullivan and K. Pruess, Analysis of injection testing of geothermal reservoirs. Transactions, Geothermal Resources Council, Vol. 4, p. 401-414, September 1980.

4. A. F. Moench, Radial steam flow in two-phase geothermal reservoirs - comparison of analytical and finite difference solutions. *Soc. Pet. Eng. J.,* October 1980, pp. 359-362.

5. M. J. O'Sullivan, A similarity method for geothermal well test analysis. *Water Resour. Res.,* Vol. 17, No. 2, p. 390-398, April 1981.

6. D. K. Woodward and R. K. M. Thambynayagam, Pressure build-up and fall-off analysis of water injection tests. Manuscript, London 1983 (to appear in SPE Formation Evaluation).

7. P. Delaney, Heating of a fully saturated Darcian half-space: pressure generation, fluid expulsion, and phase change. *Int. J. Heat Mass Transfer,* Vol. 27, No. 8, pp. 1327-1335, 1984.

8. K. S. Udell, Heat transfer in porous media considering phase change and capillarity - the heat pipe effect. *Int. J. Heat Mass Transfer,* Vol. 28, No. 2, pp. 485-495, 1985.

9. K. S. Udell and J. S. Fitch, Heat and mass transfer in capillary porous media considering evaporation, condensation, and non-condensible gas effects. Paper presented at 23rd ASME/AIChE National Heat Transfer Conference, Denver, Colorado, August 1985.

10. A. Giovannoni, G. Allegrini, G. Cappetti, and R. Celati, First results of a reinjection experiment at Larderello. Proceedings, Seventh Workshop Geothermal Reservoir Engineering, Stanford, December 1981, SGP-TR-55.

11. G. Cappetti, A. Giovannoni, C. Ruffilli, C. Calore, and R. Celati, Reinjection in the Larderello geothermal field. Proceedings, International Conference on Geothermal Energy, Firenze, BHRA Fluid Engineering, Cranfield, Bedford (England), pp. 395-408, 1982.

12. R. Bertrami, C. Calore, G. Cappetti, R. Celati, and F. D'Amore, A three-year recharge test by reinjection in the central area of Larderello field: Analysis of production data. 1985 International Symposium on Geothermal Energy, GRC Transactions, Vol. 9, Part II, pp. 293-298, 1985.

13. M. Abramowitz and I. A. Stegun, Handbook of mathematical functions. Dover, New York 1965.

14. G. Bodvarsson, Thermal problems in the siting of reinjection wells. *Geothermics,* Vol. 1, No. 2, 63-66, 1972.

15. C. Calore, K. Pruess, and R. Celati, Modeling studies of cold water injection into fluid-depleted, vapor-dominated geothermal reservoirs. Paper presented at 11th Workshop Geothermal Reservoir Engineering, Stanford University, Stanford, California, January 1986.

16. International Formulation Committee, A formulation of the thermodynamic properties of ordinary water substance. IFC Secretariat, Düsseldorf, Germany, 1967.

17. K. Pruess, Development of the general purpose simulator MULKOM. Annual Report 1982, Earth Sciences Division, report LBL-15500, Lawrence Berkeley Laboratory, 1983.

18. T. N. Narisimhan and P. A. Witherspoon, An integrated finite difference method for analyzing fluid flow in porous media. *Water Resources Research,* Vol. 12, No. 1, 57-64, 1976.

19. K. Pruess and T. N. Narasimhan, A practical method for modeling fluid and heat flow in fractured porous media. *Society of Petroleum Engineers Journal,* Vol. 25, No. 1, pp. 14-26, February 1985.

20. D. W. Peaceman, Fundamentals of numerical reservoir simulation. Elsevier, Amsterdam 1977.

21. K. Pruess, G. Bodvarsson, R. C. Schroeder, and P. A. Witherspoon, Model studies of the depletion of two-phase geothermal reservoirs. *Society of Petroleum Engineers Journal,* Vol. 22, No. 2, 280-290, April 1982.

22. R. C. Schroeder, M. J. O'Sullivan, K. Pruess, R. Celati, and C. Ruffilli, Reinjection studies of vapor-dominated systems. *Geothermics,* Vol. 11, No. 2, 93-120, 1982.

23. L. P. Dake, Fundamentals of reservoir engineering. Elsevier, Amsterdam, 1978.

APPENDIX A: Vapor Flow

We consider the flow of single-phase vapor. From the mass balance,

$$\frac{\partial \phi \rho_v}{\partial t} = - \operatorname{div} \mathbf{F}_v \tag{A.1}$$

Darcy's law,

$$\mathbf{F}_v = -k \frac{\rho_v}{\mu_v} \nabla p \tag{A.2}$$

and the real gas law,

$$pV = ZnRT \tag{A.3}$$

we have, neglecting derivatives of the compressibility factor Z

$$\frac{\phi}{p} \frac{\partial p^2}{\partial t} = \frac{k}{\mu_v} \Delta p^2 \tag{A.4}$$

An approximate linear equation in p^2 can be obtained by evaluating the coefficients at an average pressure, $\bar{p} = (p_f + p_o)/2$ [23]. Defining a diffusivity parameter

$$\alpha = \frac{\bar{p}k}{\phi \mu_v(\bar{p}, T_o)} \tag{A.5}$$

we have

$$\frac{\partial p^2}{\partial t} = \alpha \Delta p^2 \tag{A.6}$$

We seek a solution to (A.6) subject to initial conditions

$$p^2 = p_o^2 \tag{A.7}$$

and boundary conditions

$$\left. \frac{\partial p^2}{\partial r} \right|_f = - \frac{2ZRT_o \mu_v}{km} \frac{q_{vf}}{2\pi r_f H} \tag{A.8a}$$

$$\left.\frac{\partial p^2}{\partial r}\right|_{r\to\infty} = 0 \tag{A.8b}$$

The function

$$p^2(r,t) = p_o^2 - D\cdot Ei\,(-r^2/4\alpha t) \tag{A.9}$$

satisfies (A.6), (A.7), and (A.8b). From (A.8a) we have

$$D = \frac{ZRT_o\mu_v}{2\pi kHm} q_{vf} \exp\left(\frac{r_f^2}{4\alpha t}\right) \tag{A.10}$$

From the arguments presented in Section 2, we know that $x_f = r_f^2/t$, q_{vf}, and Z (T_o,p_f) are constants. Therefore, the coefficient D itself is a constant, independent of r and t, so that (A.9) is an exact solution of (A.6) through (A.8). The solution is

$$p^2 = p_o^2 - \frac{ZRT_o\mu_v}{2\pi kHm} q_{vf} \exp\left(\frac{r_f^2}{4\alpha t}\right) Ei\left(\frac{-r^2}{4\alpha t}\right) \tag{A.11}$$

APPENDIX B: Heat Balance at the Boiling Front

We develop a heat balance for a small region swept by the advancing boiling front, using simple approximations where appropriate. As the front advances from r_f to r_f+dr_f, the change in heat content of the region (r_f, $r_f + dr_f$) is, neglecting the small heat content of displaced vapor,

$$\left[(1-\phi)\,\rho_R C_R\,(T_f - T_o) + \phi\rho_l\, u_{l,f}\right] 2\pi r_f\, H\, dr_f \tag{B.1}$$

This must equal the net amount of heat and mechanical (pressure) work imparted on the region which is, neglecting heat conduction,

$$(q_l\, u_{l,f} - q_{vf}\, h_v)\, dt \tag{B.2}$$

Here we have assumed steady flow throughout the liquid region, which is an excellent approximation because of the small compressibility of liquid water. Also, we have neglected the small difference between enthalpy and internal energy for the liquid phase. Vapor is assumed to leave the front at original reservoir temperature, $h_v = h_v(T_o, p_f)$. This takes into account the heat exchange between the medium ahead of the front, and the vapor leaving the boiling surface.

To combine (B.1) and (B.2) it is necessary to consider the time dependence of the front location r_f. This can be obtained from the total liquid mass present in the injection plume, which is

$$M_l\,(t) = (q_l - q_{vf})t = \pi r_f^2 H\phi\bar{\rho}_l \tag{B.3}$$

The average liquid density is, neglecting the small pressure effects,

$$\bar{\rho}_l = \omega\rho_l\,(T_{inj}) + (1-\omega)\rho_l\,(T_f) \tag{B.4}$$

so that

$$\frac{dr_f^2}{dt} = \frac{q_l - q_{vf}}{\pi H\phi\bar{\rho}_l} \tag{B.5}$$

Equating (B.1) and (B.2), and using (B.5), we finally obtain for the temperature at the front

$$T_f = T_o - \frac{h_{vl}\,\phi\overline{\rho}_l}{(1-\phi)\,\rho_R C_R\,(q_l\,/q_{vf} - 1)} \tag{B.6}$$

Table 1. Problem Parameters

Permeability	50.E–15 m^2
Thickness	200 m
Rock grain density	2600 kg/m^3
Rock specific heat	920 J/kg °C
Reservoir temperature	240 °C
Reservoir pressure	6.0 bars
Injection enthalpy	1.258 E5 J/kg (≈29.4 °C)

Table 2. Grid for Numerical Simulations

The grid consists of concentric cylinders about $r = 0$ with height $H = 200$ m. The radii of the grid block boundaries are

$r_i = 2i$ for $i = 1, 2, ..., 50$

$r_{i+1} = fr_i$ for $i = 51, 52 ..., 100$

and $f = 1.1607...$ so that $r_{100} = 25{,}000$ m

FIGURES

Figure 1. Schematic diagram of fronts for cold water injection into a superheated vapor zone.

Figure 2. Fraction of injected fluid vaporizing.

Figure 3. Pressure and temperature of moving boiling front.

Figure 4. Simulated pressures as the boiling front propagates across a grid block (grid block #19 with 36m $\leq$ r $\leq$38m; $\phi = 8\%$, $q_l = 2$ kg/s; time step size 10^5 seconds).

Figure 5. Simulated temperatures for cold water injection into superheated vapor zone.

Figure 6. Simulated volume of liquid injection plume, compared with predictions from the analytical model.

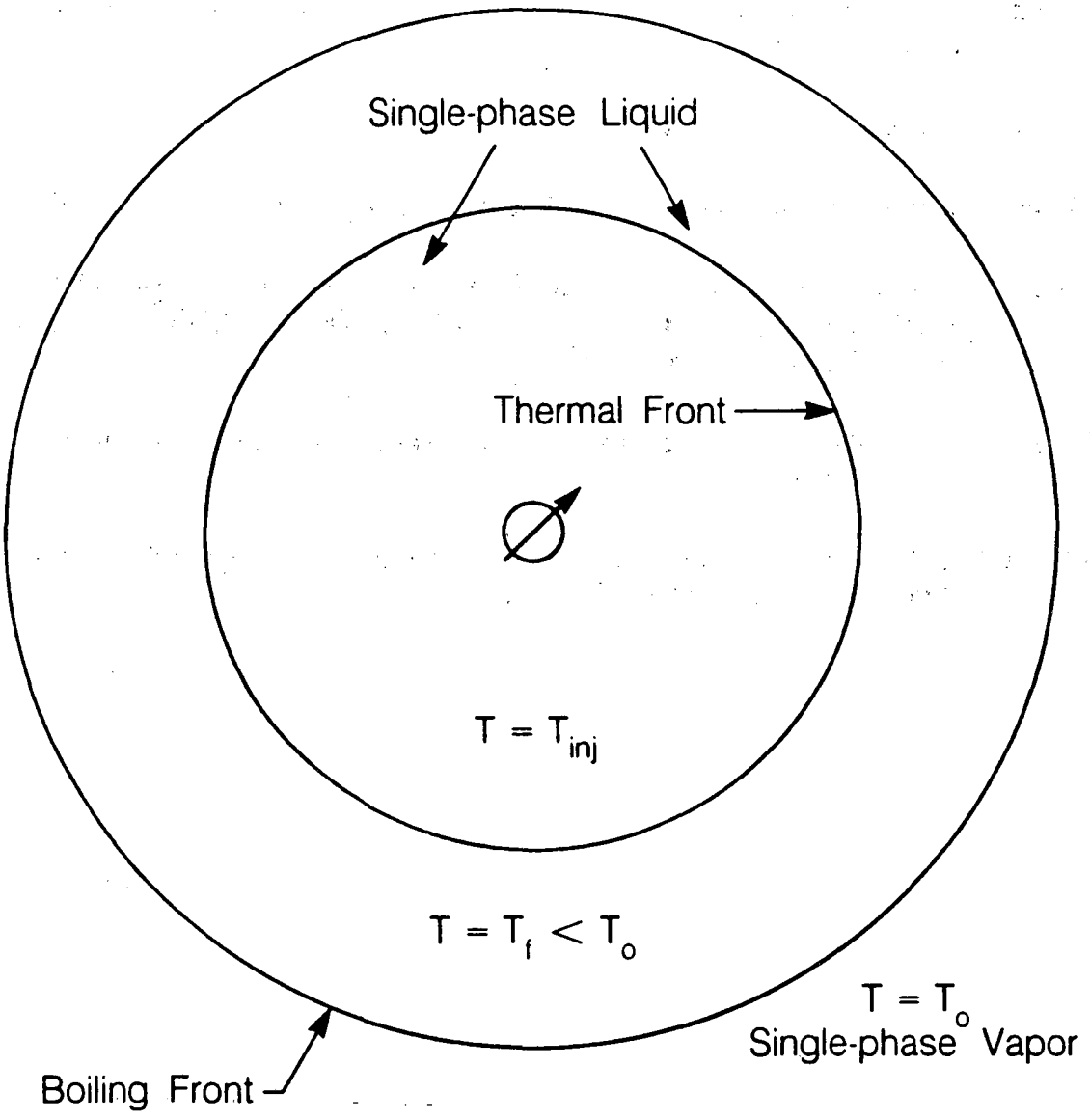

XBL 869-11015

Figure 1. Schematic diagram of fronts for cold water injection into a superheated vapor zone.

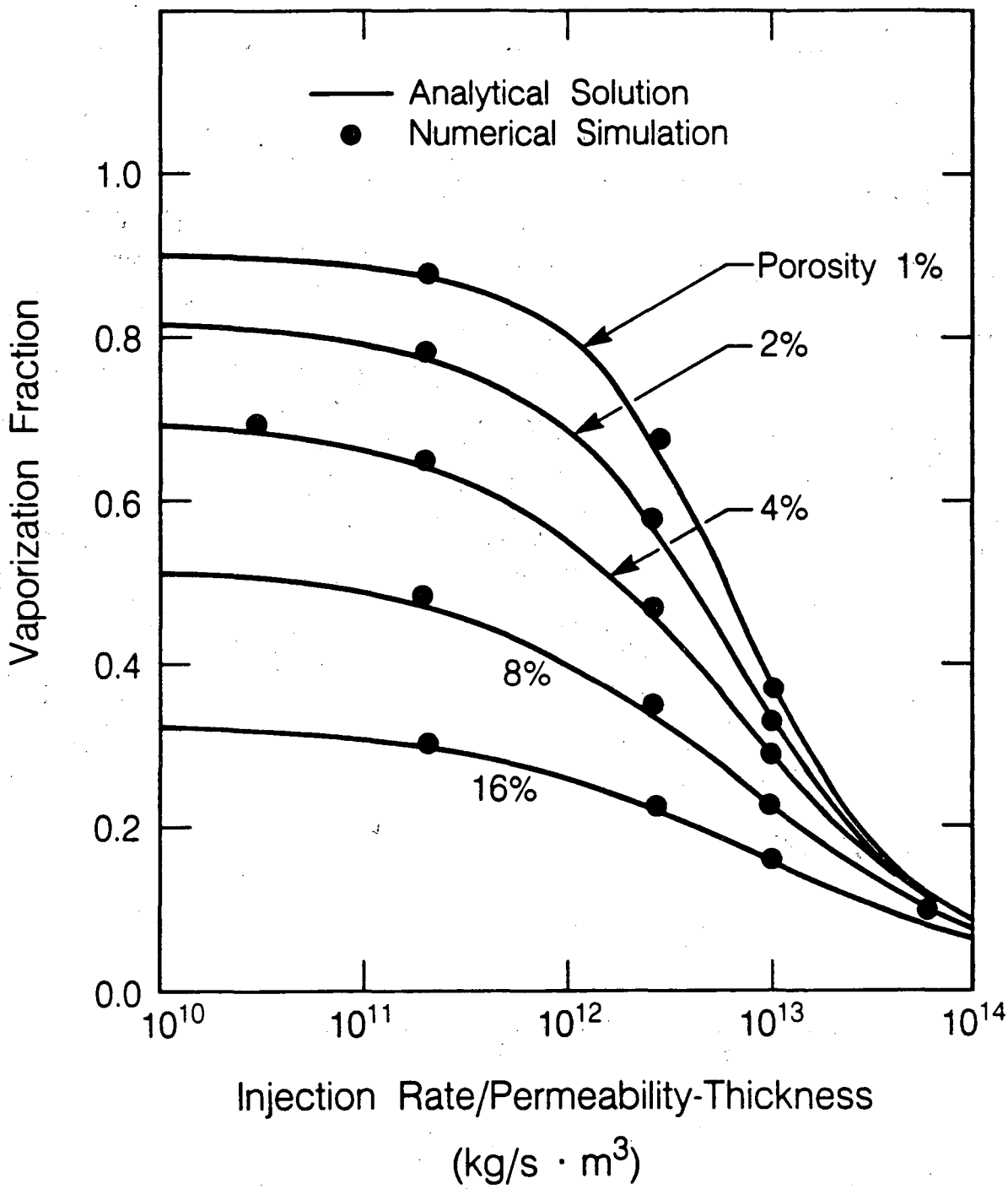

XBL 869-11017

Figure 2. Fraction of injected fluid vaporizing.

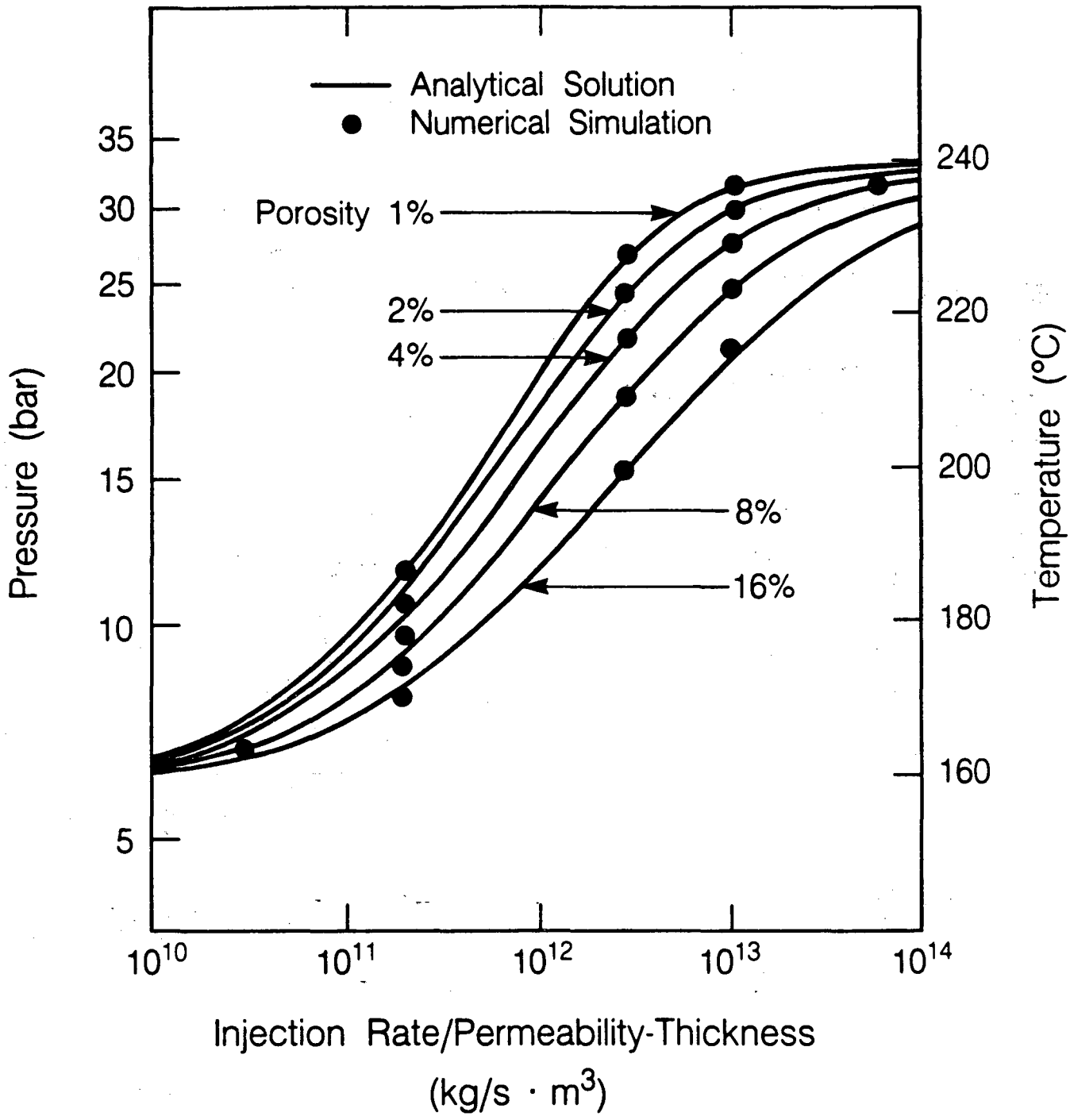

XBL 869-11018

Figure 3. Pressure and temperature of moving boiling front.

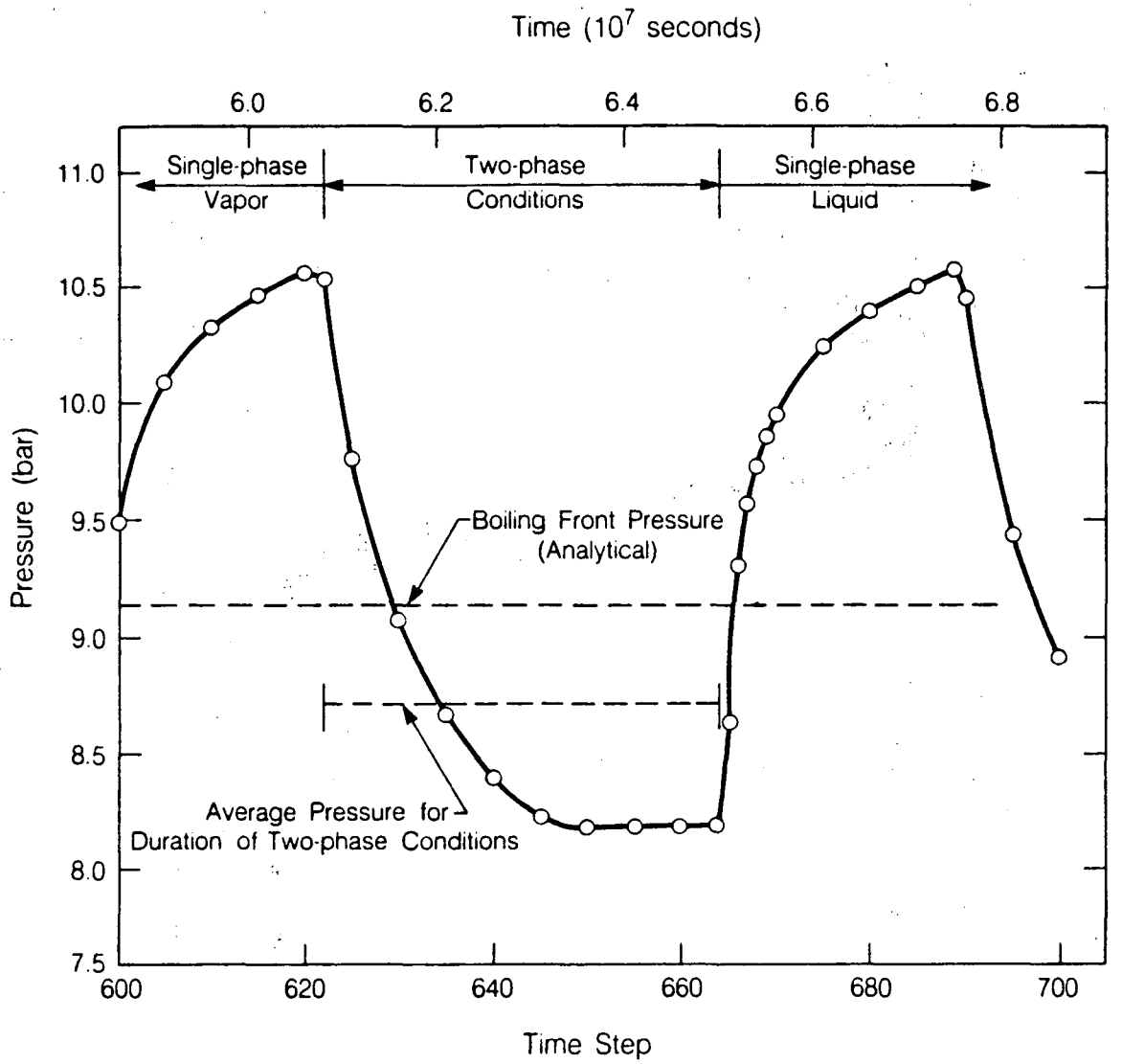

XBL 869 11016

Figure 4. Simulated pressures as the boiling front propagates across a grid block (grid block #19 with 36m $\leq$ r $\leq$38m; $\phi = 8\%$, $q_l = 2$ kg/s; time step size 10^5 seconds).

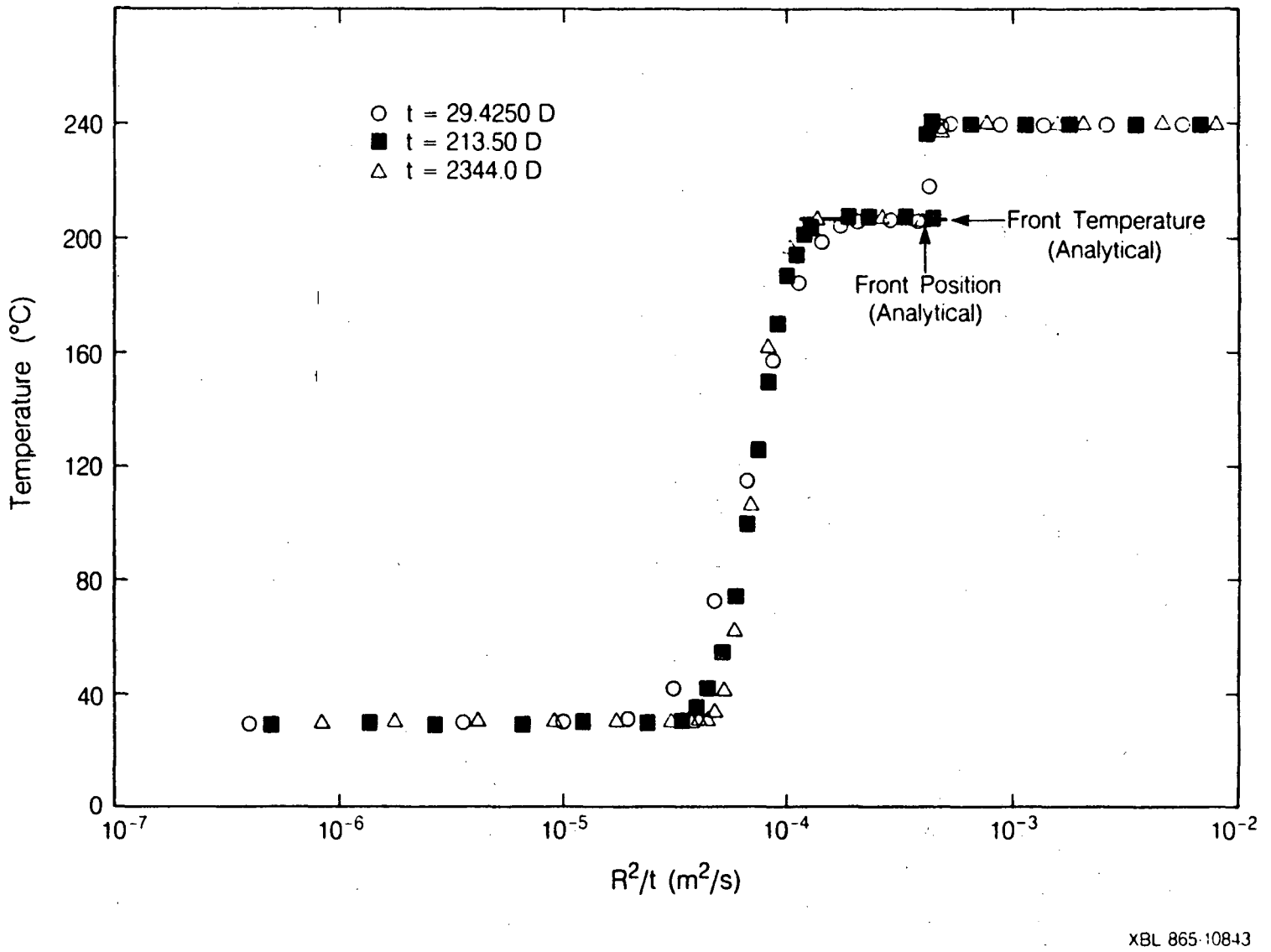

Figure 5. Simulated temperatures for cold water injection into superheated vapor zone.

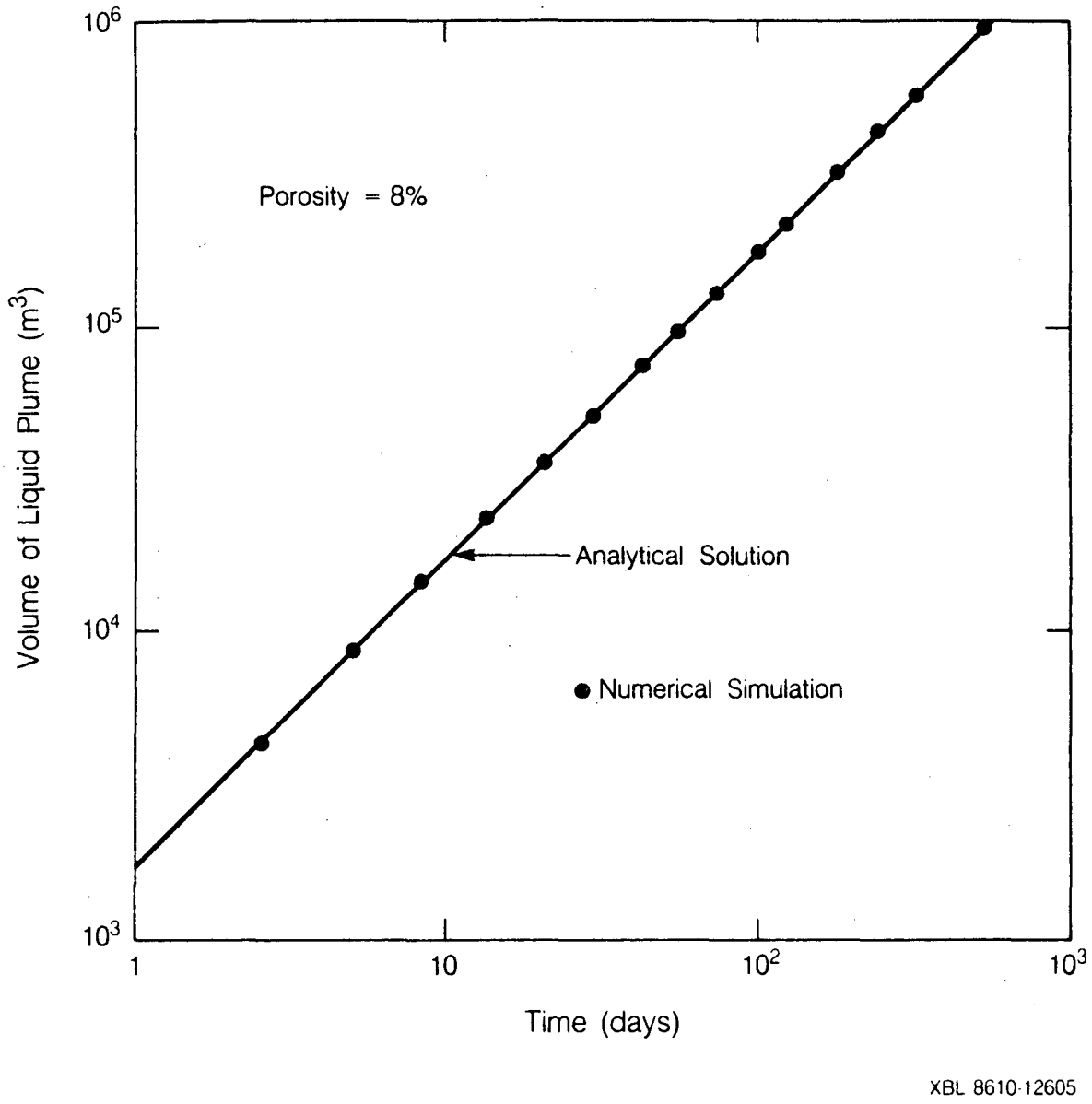

Figure 6. Simulated volume of liquid injection plume, compared with predictions from the analytical model.

This report was done with support from the Department of Energy. Any conclusions or opinions expressed in this report represent solely those of the author(s) and not necessarily those of The Regents of the University of California, the Lawrence Berkeley Laboratory or the Department of Energy.

Reference to a company or product name does not imply approval or recommendation of the product by the University of California or the U.S. Department of Energy to the exclusion of others that may be suitable.

LAWRENCE BERKELEY LABORATORY
TECHNICAL INFORMATION DEPARTMENT
UNIVERSITY OF CALIFORNIA
BERKELEY, CALIFORNIA 94720